**Solid Freeform Fabrication 2024: Proceedings of the 35th Annual International
Solid Freeform Fabrication Symposium – An Additive Manufacturing Conference
Reviewed Paper**

Prediction of Fatigue Properties of Fiber-reinforced Composites Manufactured by Material Extrusion

Mithila Rajeshirke[1], Ismail Fidan[2], Suhas Alkunte[3], and Vivekanand Naikwadi[4]

[1]Department of Engineering Technology
Middle Tennessee State University, Murfreesboro, TN 37132, USA
[2]Department of Manufacturing and Engineering Technology
Tennessee Tech University, Cookeville, TN 38505, USA
[3]Department of Mechanical Engineering Technology
Indiana State University, Terre Haute, IN 47802, USA
[4]Department of Mechanical Engineering
Tennessee Tech University, Cookeville, TN 38505, USA

Abstract

The inherent anisotropy and heterogeneity resulting from the inclusion of fibers into polymers make it challenging to predict the fatigue properties of fiber-reinforced composites manufactured by the material extrusion (MEX) process. A mathematical and computational technique, Homogenization, offers a solution by enabling the study of materials with complex microstructures. This approach allows for predicting behaviors effectively by upscaling the properties of constituent microstructural components. In this article, the fatigue properties of fiber-reinforced PETG components manufactured by MEX are predicted through a combination of homogenization and Basquin's model. The R^2 value for experimental data is 0.9752 and for homogenization analysis is 1. Such predictive methods hold promise for enhancing the performance and reliability of advanced composite materials in various engineering applications.

Keywords: Material Extrusion, Fatigue Prediction, Composites, Homogenization.

Introduction

Material Extrusion (MEX) is the most widely used and extended additive manufacturing (AM) technology [1]. MEX generates 3D objects by extruding semi-molten thermoplastic materials through heated nozzle/nozzles onto a platform. The process involves heating a thermoplastic filament to its melting point and then depositing it layer by layer to create the desired object. Various polymeric materials used for MEX include nylon, polyester, epoxy, Polyethylene Terephthalate Glycol (PETG), Polycarbonate (PC), Acrylonitrile Butadiene Styrene (ABS), Polylactide (PLA), Polyamide (PA), and others [2]. Each of these materials offers unique properties that can be leveraged depending on the requirements of the specific application, such as mechanical strength, flexibility, and thermal resistance. The versatility and accessibility of MEX have made it a popular choice in various industries, from prototyping and product development to custom manufacturing and education [3], [4]. Its ability to produce complex geometries with high precision and relatively low cost has driven significant advancements in the field of AM [5], [6], [7].

Predicting the properties of fiber-reinforced composites manufactured by MEX is difficult due to inherent anisotropy and heterogeneity because of the inclusion of fibers [8], [9]. Homogenization is a mathematical and computational technique used in the study of materials and structures with complex microstructures. It allows this study to predict the effective or macroscopic behavior of these heterogeneous materials by averaging or upscaling the properties and behaviors of their constituent microstructural components. The process of homogenization is particularly useful when dealing with materials that exhibit significant spatial variations in their properties or have multiple phases or constituents within their microstructure. These could include composites, porous media, polycrystalline materials, and other heterogeneous materials. There are two primary approaches to homogenization:

- Analytical homogenization: This method involves developing analytical expressions or closed-form solutions to calculate the effective properties of the heterogeneous material based on the properties of its individual constituents and their arrangement. This approach is usually applicable to simple microstructures or periodic arrangements.
- Numerical homogenization: Numerical homogenization methods are employed when the microstructure is too complex to yield analytical solutions. In numerical homogenization, Finite Element Methods (FEMs) and other computational techniques are used to simulate the behavior of the Representative Volume Element (RVE) under various loading conditions [10], [11]. The results of these simulations are then used to estimate the effective macroscopic properties of the material.

The basic steps in numerical homogenization include RVE generation, microscale simulation, upscaling, and validation as shown in Figure 1. RVE generation i.e., creating a RVE is a crucial step in homogenization. The RVE should be a small portion of the material that captures the essential features of the microstructure. Microscale simulations perform detailed numerical simulations on the RVE to obtain the local responses and fields (e.g., stress, strain) within the microstructure under specific boundary conditions. Based on the results from the microscale simulations, use appropriate averaging techniques (e.g., volume averaging, mean-field methods) to obtain the macroscopic or effective properties of the material in upscaling. Lastly, the validation step involves comparing the predictions of the homogenization process with experimental data to ensure the accuracy and reliability of the homogenized results. Homogenization has widespread applications in engineering and materials science. It enables engineers and researchers to study and predict the behavior of complex materials without the need for computationally expensive and time-consuming simulations at the microscale. This approach is particularly valuable for optimizing material properties and designing advanced materials with desired macroscopic behavior.

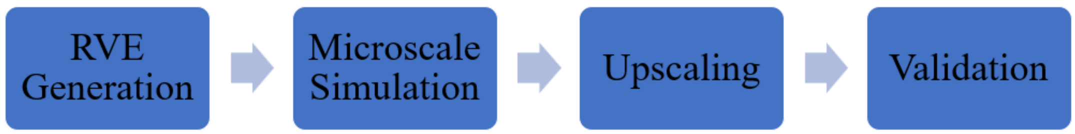

Figure 1: The basic steps in predicting fatigue life with homogenization

There are several mathematical models used to curve fit data or predict fatigue values in materials [12], [13], [14]. Among these, Basquin's model stands out for its simplicity and effectiveness, particularly when applied to fiber-reinforced composites [15]. Basquin's model can be represented by the equation (1). Where S is the tensile stress, N_f is cycles to failure, and A and b are material constants. Basquin's model is highly valued in material science and engineering due to its straightforward nature and the ability to accurately predict the fatigue behavior of composites. By correlating stress with the number of cycles to failure, it provides a reliable method for estimating the lifespan of materials under cyclic loading. The constants A and b are material-specific, enabling accurate customization and prediction. These constants are determined experimentally and are also applied to the homogenization curve. In addition to its application to fiber-reinforced composites, Basquin's model is also utilized across various other materials and industries due to its robustness and adaptability. This model aids engineers and researchers in designing and evaluating materials that must withstand repeated loading, ensuring safety and performance in practical applications.

$$s = A \cdot N_f^b \tag{1}$$

In recent literature, there has been a significant emphasis on improving RVE generation techniques to enhance the accuracy and efficiency of FEM-based homogenization. Some studies focus on automating the RVE generation process through Machine Learning algorithms or Genetic Algorithms, enabling faster and more reliable simulations [16]. Additionally, researchers are exploring ways to integrate multiscale modeling approaches, where multiple levels of material behavior are simulated instantaneously [16], [17], [18]. This allows for a more comprehensive understanding of how microstructural features influence the material's overall response. Moreover, advancements in parallel computing and high-performance computing have facilitated the simulation of larger and more complex RVEs, enabling researchers to capture finer details of the material's microstructure and achieve more accurate predictions of its mechanical behavior. There are very few studies that have reported the prediction of mechanical properties with the aid of FEM and RVE in the field of AM. Korshunova et al. presented image-based numerical characterization and experimental validation of the tensile behavior of octet-truss lattice structures [19]. Sharafi et al. proposed a dual-scale material model to predict the influence of various processing parameters on the macroscale deformation using the commercial software packages, Digimat, to model the microscopic behavior and ANSYS to predict the macroscopic response [20]. RVE with the Mori-Tanaka homogenization approach is used to predict the maximum stress and deflection at failure for the entire part. Nasirov et al. investigated the homogenization approach as a tool for predicting the mechanical properties of FDM-printed parts and examined the postprocessing possibility of microscale displacements, strains, and stresses [21]. Furthermore, Spina et al. have also researched the effective mechanical behavior of structural elements of an FFF component with a multiscale analysis. The development and validation of a homogenization model using a material with elastoplastic properties and Hill's yield criterion is presented [22]. In this paper, the homogenization technique through the Workbench tool is utilized including RVE generation. The predicted mechanical tensile properties obtained from the Workbench tool are integrated into Basquin's model to validate their accuracy and reliability in predicting fatigue properties.

Materials And Methods

For homogenization, the basic material properties for PETG and Short carbon fiber (SCF) were incorporated into ANSYS Material Designer (MD). The material properties of PETG and SCF are shown in Table 1 and Table 2. The two-scale homogenization was utilized for this research as depicted in Figure 2. The 3D-printed composites underwent homogenization using the ANSYS MD software. Initially, the neat material inputs were defined in the Engineering Data and MD module, which were subsequently placed into the Workbench workspace via drag and drop.

Table 1: The material properties of PETG

Properties	Values
Density	1270 kg/m3
Young's Modulus	1.72E+09 Pa
Poisson's Ratio	0.48
Bulk Modulus	1.4333E+10 Pa
Shear Modulus	5.8108E+08 Pa
Tensile Yield Strength	4.7E+07 Pa

Table 2: The material properties of SCF

Properties	Values
Density	1800 kg/m3
Young's Modulus X direction	2.4E+11 Pa
Young's Modulus Y direction	2.4E+10 Pa
Young's Modulus Z direction	2.4E+10 Pa
Poisson's Ratio XY	0.2
Poisson's Ratio YZ	0.4

Poisson's Ratio XZ	0.2
Shear Modulus XY	9E+09 Pa
Shear Modulus YZ	8.214E+09 Pa
Shear Modulus XZ	9E+09 Pa

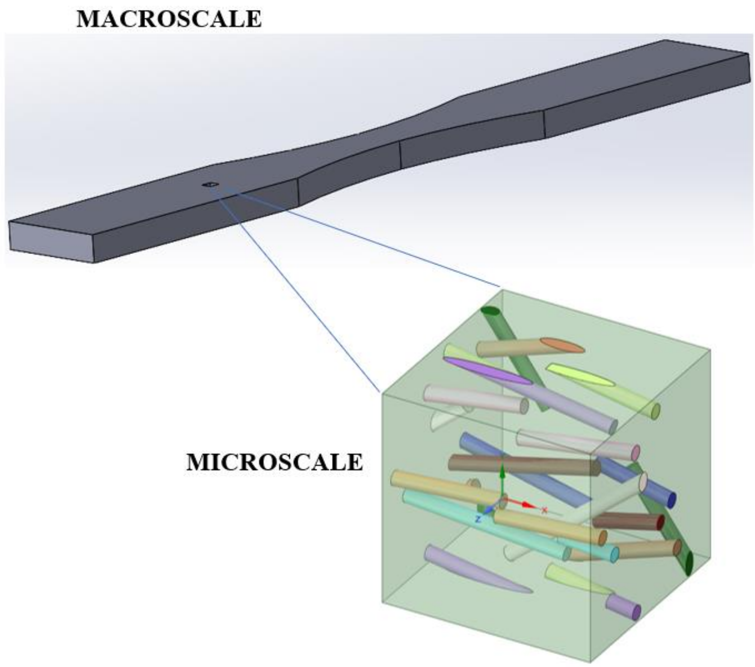

Figure 2: Two-scale homogenization

The homogenization process involved analyzing microscale RVEs of the composite. RVE is generated as shown in Figure 3. These computed matrices were then utilized for macroscale homogenization. Microscale RVE meshing involved employing both conformal and periodic meshing techniques as shown in Figure 4. After computing, the engineering constants/material constants are obtained as a result as shown in Figure 5, which then is fed as input further for the static structural tool. In the static structural tool, tensile properties are determined at the macroscopic level. The macroscale tensile specimen geometry was designed in SolidWorks and then exported in IGES file format for ANSYS meshing as given in Figures 6 and 7 respectively. Meshing was performed using quadrilateral linear elements with a 0.5 mm element size. Fixed support and force of 3550 N applied are shown in Figure 8. After computing, the tensile strength is obtained for the SCF-PETG specimen, and this property is then given as input to Basquin's equation.

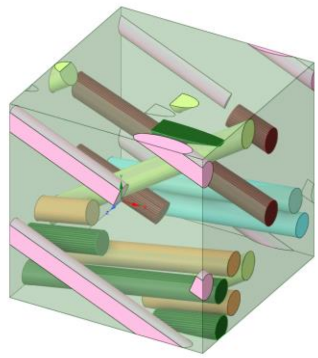

Figure 3: RVE Generation

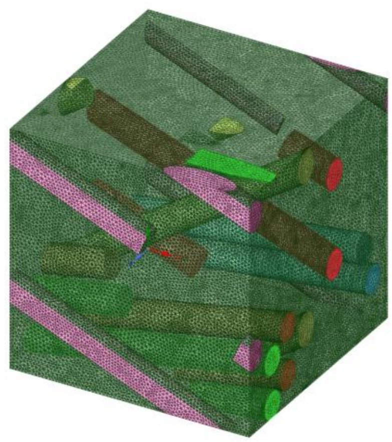

Figure 4: Meshing of RVE

Name	Value	Unit	P
Engineering Constants			
E1	7454.1	MPa	☐
E2	2173.7	MPa	☐
E3	2420	MPa	☐
G12	1135.4	MPa	☐
G23	609.94	MPa	☐
G31	621.6	MPa	☐
nu12	0.67385		☐
nu13	0.28591		☐
nu23	0.73018		☐
Density			
rho	1.3286E-09	t mm^-3	☐
Logs			
RVE log			
Solver logs			

Figure 5: Engineering constants / Material Constants

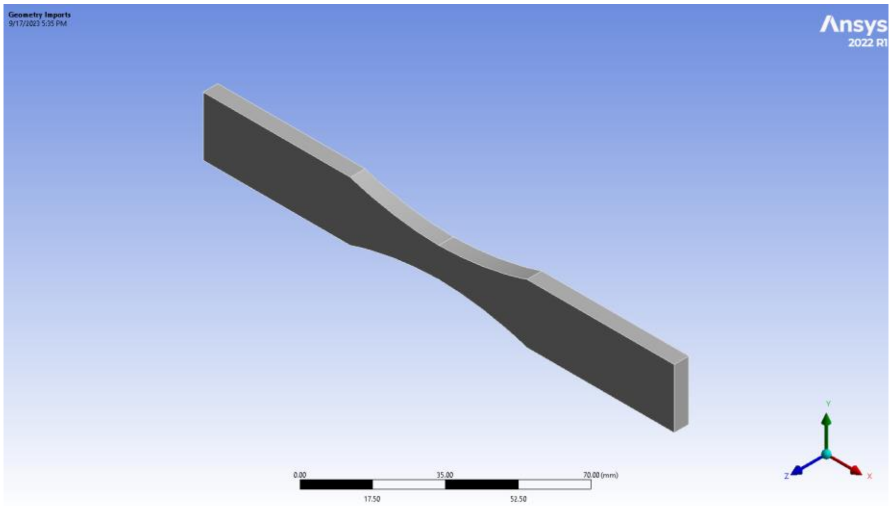

Figure 6: Geometry of the specimen

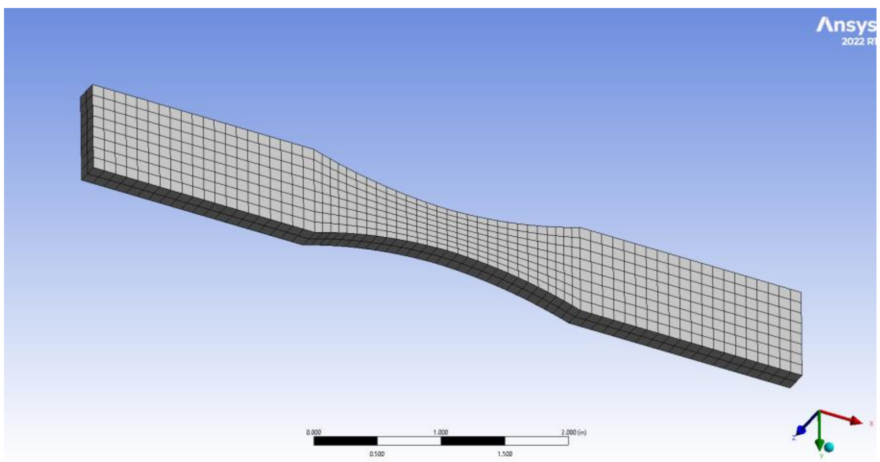

Figure 7: Periodic meshing applied

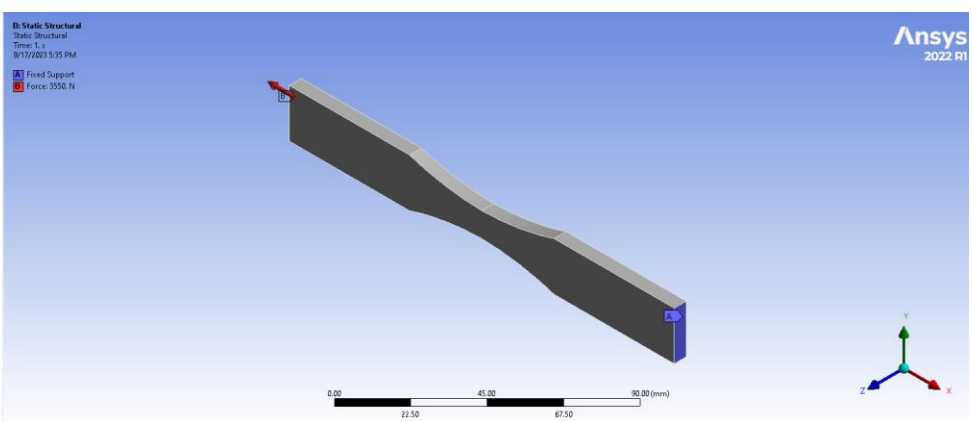

Figure 8: Fixed support and force applied

For validation study with experimental data, specimens were printed with the geometry chosen for the research based on the ISO 11782-1:1998(E) standard [23], as illustrated in Figure 9. SCF PETG material was used from a Push Plastic manufacturer [24]. A CAD model was created using SolidWorks and saved in STL format. This STL file was then imported into PRUSA slicing software, where the printing parameters such as infill density 100%, infill pattern align rectilinear/unidirectional laminate [0°]50, nozzle diameter 0.4 mm, nozzle temperature 240°C, bed temperature 90°C, layer height 0.05 mm, and infill angle 0° were configured. The software generated a G-code, which the PRUSA i3 MK3 printer used to print the specimens.

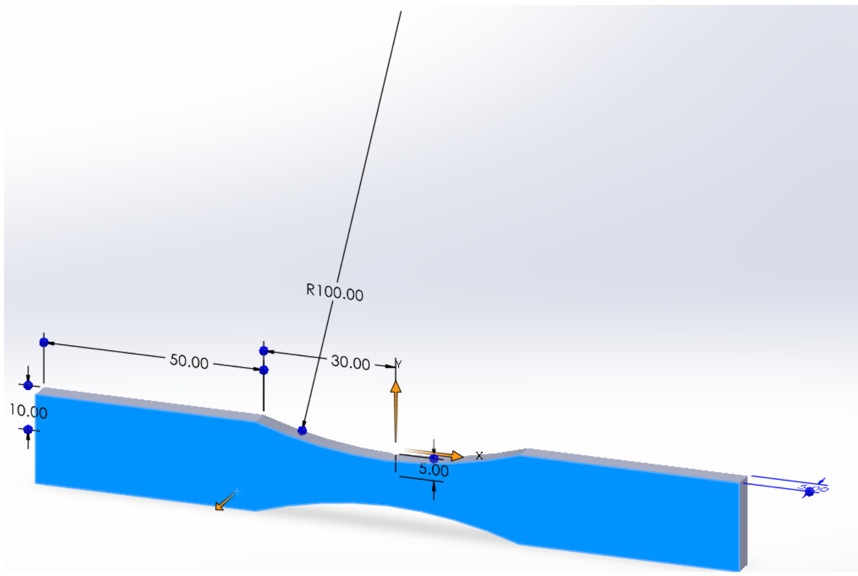

Figure 9: Specimen geometry (All dimensions are in mm)

The ultimate tensile strength (UTS) is determined by conducting static tensile tests with a strain rate of 5 mm/min on the three replicates of specimens with the 810E4-15 Dynamic Test System, and then the average is taken as UTS. The result of tensile tests is presented in Table 3. After getting UTS, the fatigue characteristics of the material were assessed using the same machine. Testing was conducted under tensile-tensile conditions with a stress ratio of 0.1. Four different stress levels were selected for the study, with three specimens tested at each level for fatigue analysis, as outlined in Table 3. The tests were performed at a frequency of 3 Hz, under controlled environmental conditions of 54-61% humidity and temperatures ranging from 19-23°C. The Newton test machine controller/software was used to manage test parameters, with Proportional/Integral/Derivative (PID) values set for precise waveform control, using proportional values of 1100-1400, an integral value of 100, and a derivative value of 0. The results are presented in S-N curve format as shown in Figure 11. The S-N curve was generated using a power curve fit in Excel, which helped determine the material constants A and b for Basquin's equation. Once these parameters were established, the equation was applied to the UTS obtained from homogenization. For four different stress levels - 65 MPa, 60 MPa, 55 MPa, and 46 MPa—the number of cycles was predicted. Subsequently, the curve was fitted using a power curve in Excel for further analysis.

Table 3: Stress Levels

Stress Level	Maximum Stress (MPa)	Minimum Stress (MPa)
1	66	6.6
2	56	5.6
3	52	5.2
4	46	4.6

<u>Result and Discussion</u>

The UTS value is determined from the homogenization analysis and incorporated to form an S-N curve by using Basquin's equation. The tensile strength result is shown in Figure 10. The comparison of experimental and homogenized results is shown in Table 4. The UTS value induced in the experimental set-up for commercial filament [25], layer height 0.05 mm, unidirectional laminate [0°]50 is 71.05 MPa when 3552 N load was applied. In ANSYS workbench, static structural analysis the force is applied as 3550 N, and the maximum stress was determined with Maximum Principal Stress theory. The obtained value for ultimate stress was 80.77 MPa from ANSYS. For the validation study, the value obtained in homogenization for the tensile test and the material constants A and b are then given as input to Basquin's model to get the S-N curve as shown in Figure 11. The R^2 value for experimental data is 0.9752 and for homogenization analysis is 1 as given in Figure 11. In this case, the experimental data has a strong correlation, while the homogenization analysis shows a perfect fit, suggesting highly accurate predictions in the homogenization model.

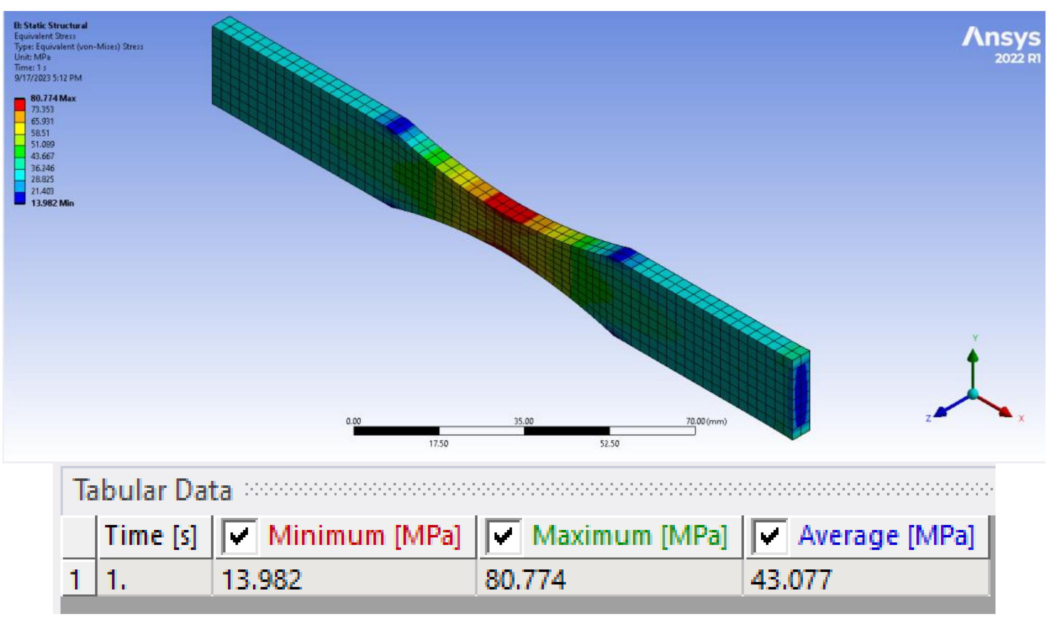

	Time [s]	Minimum [MPa]	Maximum [MPa]	Average [MPa]
1	1.	13.982	80.774	43.077

Figure 10: Results for Ultimate Tensile Strength

Table 4: Comparison of experimental and homogenized results

Parameters	Homogenization Values	Experimental Values
Force Applied	3550 N	3552 N
Equivalent Max. Stress / Ultimate Tensile stress	80.77 MPa	71.05 MPa

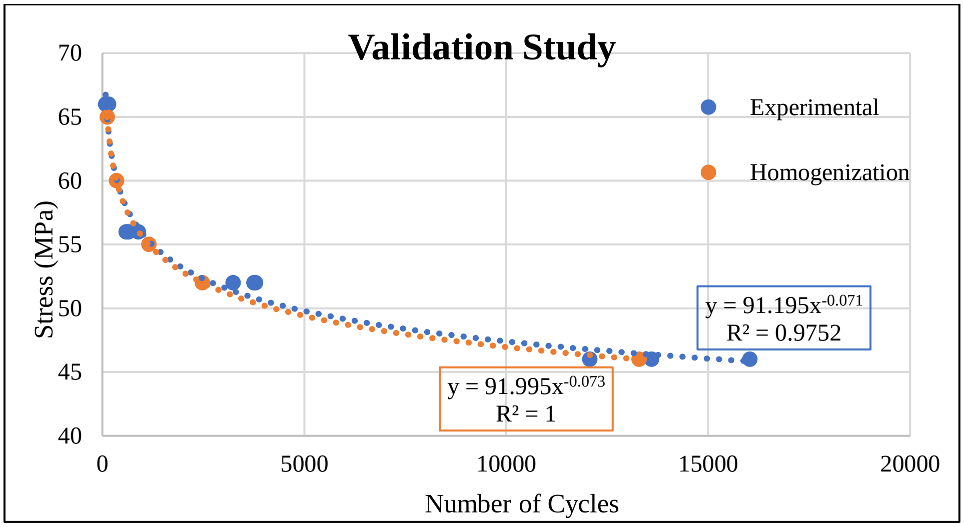

Figure 11: Validation of the fatigue result for experimental and homogenization analysis

Conclusions

In this study, we utilized the homogenization technique via the Workbench tool, including RVE generation, to predict the mechanical tensile properties of SCF-PETG composite components produced by MEX. These predicted properties were incorporated into Basquin's model to assess their accuracy in forecasting fatigue behavior. The integration of homogenization results with Basquin's model effectively predicted the fatigue life of these composite components. This approach demonstrates that, with known tensile strength of fiber-reinforced composites and Basquin's model constants, fatigue life can be accurately estimated. It successfully bridges the gap between numerical simulations and empirical modeling, providing valuable insights into the fatigue behavior of SCF-PETG composites under cyclic loading.

Acknowledgements

This research has been funded by the Center for Manufacturing Research and the Department of Mechanical Engineering of Tennessee Tech University. The authors appreciate the provided funding.

References

[1] M. Rajeshirke, I. Fidan, A. Gupta, and K. Mäntyjärvi, "Fatigue Analysis of Short Carbon Fiber Reinforced Composite Components Manufactured Using Fiber-Reinforced Additive Manufacturing," 2022, doi: 10.26153/TSW/44139.

[2] S. Hasanov, S. Alkunte, M. Rajeshirke, A. Gupta, O. Huseynov, I. Fidan, F. Alifui-Segbaya, A. Rennie, 'Review on Additive Manufacturing of Multi-Material Parts: Progress and Challenges. Journal of Manufacturing and Materials Processing.' (2022); 6(1):4. https://doi.org/10.3390/jmmp6010004".

[3] J. M. Pearce *et al.*, "Recent Inventions in Additive Manufacturing: Holistic Review," *Inventions 2023, Vol. 8, Page 103*, vol. 8, no. 4, p. 103, Aug. 2023, doi: 10.3390/INVENTIONS8040103.

[4] M. A. Ali, I. Fidan, and K. Tantawi, "Investigation of the impact of power consumption, surface roughness, and part complexity in stereolithography and fused filament fabrication," *International Journal of Advanced Manufacturing Technology*, vol. 126, no. 5–6, 2023, doi: 10.1007/s00170-023-11279-3.

[5] I. Fidan, P. Fidan, S. S. Alkunte, O. Huseynov, M. A. Ali, and V. A. Naikwadi, "Unique Instructional Delivery of Additive Manufacturing: A Holistic Review," *2024 ASEE Annual Conference & Exposition Proceedings*, Jun. 2024, doi: 10.18260/1-2--48204.

[6] I. Fidan *et al.*, "Recent Inventions in Additive Manufacturing: Holistic Review," *Inventions 2023, Vol. 8, Page 103*, vol. 8, no. 4, p. 103, Aug. 2023, doi: 10.3390/INVENTIONS8040103.

[7] F. Alifui-Segbaya, I. F. Ituarte, S. Hasanov, A. Gupta, and I. Fidan, "Opportunities and Limitations of Additive Manufacturing," *Springer Handbooks*, vol. Part F1592, pp. 125–143, 2023, doi: 10.1007/978-3-031-20752-5_9.

[8] A. Nasirov and I. Fidan, "Prediction of mechanical properties of fused filament fabricated structures via asymptotic homogenization," *Mechanics of Materials*, vol. 145, p. 103372, Jun. 2020, doi: 10.1016/J.MECHMAT.2020.103372.

[9] S. Hasanov, A. Gupta, F. Alifui-Segbaya, and I. Fidan, "Hierarchical homogenization and experimental evaluation of functionally graded materials manufactured by the fused filament fabrication process," *Compos Struct*, vol. 275, p. 114488, Nov. 2021, doi: 10.1016/J.COMPSTRUCT.2021.114488.

[10] S. BELHOUİDEG, "Prediction of effective mechanical properties of composite materials using homogenization approach: Application to tungsten fiber reinforced bulk metallic glass matrix composite," *European Mechanical Science*, vol. 2, no. 2, pp. 68–75, Jun. 2018, doi: 10.26701/EMS.376369.

[11] A. El Moumen, M. Tarfaoui, and K. Lafdi, "Additive manufacturing of polymer composites: Processing and modeling approaches," *Compos B Eng*, vol. 171, pp. 166–182, Aug. 2019, doi: 10.1016/J.COMPOSITESB.2019.04.029.

[12] S. Alkunte, M. Rajeshirke, I. Fidan, and S. Hasanov, "Performance evaluation of fatigue behavior in extrusion-based functionally graded materials," *International Journal of Advanced Manufacturing Technology*, pp. 1–13, Jul. 2023, doi: 10.1007/S00170-023-11922-Z/METRICS.

[13] "M. Rajeshirke, S. Alkunte, O. Huseynov, I. Fidan, Machine Learning-Assisted Prediction of Fatigue Behaviour in Fiber-Reinforced Composites Manufactured via Material Extrusion, Proceedings of the SFF2023-34rd Annual International Solid Freeform Fabrication Symposium-An Additive Manufacturing Conference, Austin, Texas, August 14-16, 2023. ".

[14] S. Alkunte, M. Rajeshirke, O. Huseynov, and I. Fidan, "Fatigue Life Prediction of Functionally Graded TPU and PLA Components Produced by Material Extrusion," 2023, doi: 10.26153/TSW/50923.

[15] M. Rajeshirke, S. Alkunte, O. Huseynov, and I. Fidan, "Fatigue analysis of additively manufactured short carbon fiber-reinforced PETG Components," *International Journal of Advanced Manufacturing Technology*, 2023, doi: 10.1007/S00170-023-12107-4.

[16] X. Liu, D. Furrer, J. Kosters, and J. Holmes, "Vision 2040 : A Roadmap for Integrated, Multiscale Modeling and Simulation of Materials and Systems," *Contractor Report*, no. March, 2018.

[17] J. Fish, G. J. Wagner, and S. Keten, "Mesoscopic and multiscale modelling in materials," 2021. doi: 10.1038/s41563-020-00913-0.

[18] M. F. Horstemeyer, *Integrated Computational Materials Engineering (ICME) for Metals: Using Multiscale Modeling to Invigorate Engineering Design with Science*. 2012. doi: 10.1002/9781118342664.

[19] N. Korshunova *et al.*, "Image-based numerical characterization and experimental validation of tensile behavior of octet-truss lattice structures".

[20] S. Sharafi, M. H. Santare, J. Gerdes, and S. G. Advani, "A multiscale modeling approach of the Fused Filament Fabrication process to predict the mechanical response of 3D printed parts," *Addit Manuf*, vol. 51, 2022, doi: 10.1016/j.addma.2022.102597.

[21] A. Nasirov, S. Hasanov, and I. Fidan, "Prediction of mechanical properties of fused deposition modeling made parts using multiscale modeling and classical laminate theory," in *Solid Freeform Fabrication 2019: Proceedings of the 30th Annual International Solid Freeform Fabrication Symposium - An Additive Manufacturing Conference, SFF 2019*, 2019.

[22] R. Spina, B. Cavalcante, S. Di Rosa, G. Morandina, and A. Mellone, "Multiscale modelling of additive tensile test specimens," *Procedia CIRP*, vol. 118, pp. 777–780, Jan. 2023, doi: 10.1016/J.PROCIR.2023.06.133.

[23] "ISO 11782-1:1998 - Corrosion of metals and alloys — Corrosion fatigue testing — Part 1: Cycles to failure testing." Accessed: Jul. 19, 2023. [Online]. Available: https://www.iso.org/standard/1865.html

[24] "Push Plastic 3D Printer Filament Made in the USA by Push Plastic." Accessed: Nov. 27, 2023. [Online]. Available: https://www.pushplastic.com/

[25] "Push Plastic 3D Printer Filament Made in the USA by Push Plastic." Accessed: Nov. 27, 2023. [Online]. Available: https://www.pushplastic.com/